fractal and fractional

Article

Event-Triggered Adaptive Fuzzy Control for Strict-Feedback Nonlinear FOSs Subjected to Finite-Time Full-State Constraints

Changhui Wang *, Wencheng Li and Mei Liang *

School of Electromechanical and Automotive Engineering, Yantai University, 32 Qingquan Road, Laishan District, Yantai 264005, China; liwenc97@126.com
* Correspondence: wang_changhui@126.com (C.W.); mmglm@163.com (M.L.)

Abstract: In this article, an event-triggered adaptive fuzzy finite-time dynamic surface control (DSC) is presented for a class of strict-feedback nonlinear fractional-order systems (FOSs) with full-state constraints. The fuzzy logic systems (FLSs) are employed to approximate uncertain nonlinear functions in the backstepping process, the dynamic surface method is applied to overcome the inherent computational complexity from the virtual controller and its fractional-order derivative, and the barrier Lyapunov function (BLF) is used to handle the full-state constraints. By introducing the finite-time stability criteria from fractional-order Lyapunov method, it is verified that the tracking error converges to a small neighborhood near the zero and the full-state constraints are satisfied within a predetermined finite time. Moreover, reducing the communication burden can be guaranteed without the occurrence of Zeno behavior, and the example is given to demonstrate the effectiveness of the proposed controller.

Keywords: fractional-order systems; fuzzy systems; event-triggered control; finite-time; state constraints

Citation: Wang, C.; Li, W.; Liang, M. Event-Triggered Adaptive Fuzzy Control for Strict-Feedback Nonlinear FOSs Subjected to Finite-Time Full-State Constraints. *Fractal Fract.* **2024**, *8*, 160. https://doi.org/10.3390/fractalfract8030160

Academic Editors: Norbert Herencsar, Velusamy Vijayakumar and Chendrayan Dineshkumar

Received: 9 February 2024
Revised: 26 February 2024
Accepted: 4 March 2024
Published: 12 March 2024

1. Introduction

The fractional-order systems (FOSs) with infinite memory and genetic characteristics can describe the more nonclassic phenomenon in the physical systems [1,2], which have been applied in a lot of different areas such as secret communication [3,4], vehicle [5,6], circuit [7,8], finance [9,10], image [11–13], etc.

Many nonlinear controller results for FOSs have been presented including adaptive backstepping control, dynamic surface control (DSC), and so on. Among them, the adaptive backstepping control technology can settle the tracking control problem of FOSs with mismatched conditions, in which the approximation performance of neural networks (NNs) or fuzzy logic systems (FLSs) [14–19] are always used to handle unknown nonlinear functions in the FOSs, and the stability of the closed-loop system is accomplished. For example, the authors in [20] consider nonlinear FOSs under actuator faults and come up with a NN backstepping control scheme by using the property of NNs. An adaptive fuzzy control strategy for nonstrict-feedback nonlinear large-scale FOSs is designed and analyzed in [21]. Liu et al. [22] investigate the adaptive DSC for a class of parametric uncertain FOSs by utilizing backstepping mechanism. Despite many literatures and achievements have been obtained and published, output or state constraints are ignored and not considered there.

In fact, state constraints or output constraint are the most important factor restricting system performance, and generally widespread in plentiful physical systems. Once violate these constraints at some point of the operation, the control systems are unable to work normally and cause extreme harm. To address the constraint issue to guarantee the steady-state and transient behavior of the FOSs, the barrier Lyapunov function (BLF) by employing the relevant error constraints is the prevalent method to indirectly restrict system states, and a number of the constraint control strategies for FOSs has been achieved. The authors in [23] develop an adaptive NN constraint control strategy for uncertain nonlinear nonstrict-feedback FOSs under full-state constraints, and all the states remain in their constraint bounds by introducing the BLF. In [24], a bipartite consensus of multiple nonlinear FOSs with output constraints is assessed, and a distributed backstepping control method is developed, in which the BLFs are applied to restrict the output of followers into the preset range. To achieve the performance of the FOSs under asymmetric time-varying state constraints and input nonlinearities [25], a neural adaptive DSC is proposed by using asymmetric BLFs to refrain from the transgression of the pseudo-state constraints. The uncertain nonstrict-feedback incommensurate FOSs under output constraints is addressed in [26], and an adaptive NN controller based on the observer is proposed to guarantees the tracking error satisfying the constraints. In these traditional time-trigger schemes, the communication is performed periodically, leading to the waste of resources from the communications burden and vast data transmission.

Different from time-driven periodic sampling mechanism with fixed frequency, the frequency of event-driven control (ETC) is determined according to state error, which can save communication resources and computing resources of the system, and event-triggered control for FOSs have been proposed in some outstanding works. In [27], the ETC strategy for the FOSs has been designed to ensure the stability of the closed-loop system. For fractional-order multiagent networks in [28], a distributed ETC is designed to address the limitations of communication resources. In [29], an adaptive NN ETC for FOSs with unmodeled dynamics is proposed by using Mittag-Leffler input-to-state practical stability Lyapunov function. The authors in [30] research the state estimation of the fractional-order complex networked systems with randomly occurring nonlinearities, and an adaptive nonfragile state estimation method with event-triggered mechanism is designed. For nonlinear FOSs with uncertainty and disturbance in [31], the adaptive event-triggered fuzzy DSC strategy is investigated to reduce the transmission of control signals. In [32], the adaptive NN backstepping ETC algorithm for the nonlinear double-integrator FOSs with unknown dynamics and disturbances is presented. For nonstrict-feedback uncertain multi-input multi-output time-delay FOSs with actuator faults, the observer-based adaptive hybrid fuzzy controller via dynamic surface method and event-triggered mechanism is proposed in [33]. To our best knowledge, there is a lack of research on the finite-time state constrained ETC strategy for nonlinear FOSs.

In this article, the event-triggered finite-time adaptive control method for nonlinear FOSs with actuator saturation and full-state constraints is proposed, and the major innovations are given as follows:

(1) Compared with state constrained controller [23,25,27,34] or finite-time controller for nonlinear FOSs [35–38], an event-triggered adaptive fuzzy finite-time DSC approach for strict-feedback uncertain nonlinear FOSs with actuator saturation and full-state constraints is proposed, in which the fuzzy logic systems are employed to approximate uncertain nonlinear functions in the backstepping process and the dynamic surface method is applied to overcome the inherent computational complexity from the virtual controller.

(2) Compared with the results in [39,40], the event-triggered mechanism is designed together with finite-time full-state constrained adaptive controller, and the finite-time stability of the closed-loop systems is proved based on fractional-order Lyapunov criterion, which reduces the consumption of network resources to make the proposed controller more general for application.

2. Problem Formulations and Preliminary

2.1. Systems Dynamics and Some Basic Assumptions

The following strict-feedback nonlinear FOSs with actuator saturation are considered:

$$\begin{cases} D^{\alpha}x_i = f_i(\underline{x}_i) + g_i(\underline{x}_i)x_{i+1}, i = 1,2,\ldots,n-1 \\ D^{\alpha}x_n = f_n(x) + g_n(x)u(v) \\ y = x_1 \end{cases} \quad (1)$$

where $\underline{x}_i = \begin{pmatrix} x_1 & x_2 & \dots & x_i \end{pmatrix}^{\mathrm{T}} \in R^i (i = 1, 2, \dots, n-1)$ and $x = \begin{pmatrix} x_1 & x_2 & \dots & x_n \end{pmatrix}^{\mathrm{T}} \in R^n$ are state vectors, $y \in R$ is output, $f_i(\cdot)$ is unknown function, and $g_i(\cdot)$ is known function, $i = 1, 2, \dots, n$. α is fractional order, and α^{th} is the Caputo fractional derivative of continuous function $\xi(t)$, which is defined as [41,42]:

$$D_{t_0}^{\alpha} \xi(t) = \frac{1}{\Gamma(n-\alpha)} \int_{t_0}^{t} (t-\tau)^{n-\alpha-1} \xi^{(n)}(\tau) d\tau \tag{2}$$

where $\Gamma(\alpha) = \int_0^{\infty} e^{-t} t^{\alpha-1} dt$, $n-1 < \alpha < n, n \in Z^+$. $D_{t_0}^{\alpha}$ is denoted as D^{α}, when $t_0 = 0$.

Define an open set as $\Omega_i = \{x_i(t) \in R \| x_i| < k_{c_i}, k_{c_i} > 0\}$, then each system state x_i is constrained in Ω_i. v is the control input, and $u(v)$ is the saturation input defined as:

$$u(\nu) = \begin{cases} u_{\max}, & \nu \geq u_{\max} \\ \nu, & u_{\min} < \nu < u_{\max} \\ u_{\min}, & \nu \leq u_{\min} \end{cases} \tag{3}$$

where $u_{\max} > 0$ and $u_{\min} < 0$. Saturation (3) can be described as the smooth function as follow [43,44]:

$$u(\nu) = h(\nu) + \Delta(\nu) \tag{4}$$

where

$$h(\nu) = \begin{cases} u_{\max} \cdot \dfrac{e^{\frac{\nu}{u_{\max}}} - e^{-\frac{\nu}{u_{\max}}}}{e^{\frac{\nu}{u_{\max}}} + e^{-\frac{\nu}{u_{\max}}}}, & \nu \geq 0 \\ u_{\min} \cdot \dfrac{e^{\frac{\nu}{u_{\min}}} - e^{-\frac{\nu}{u_{\min}}}}{e^{\frac{\nu}{u_{\min}}} + e^{-\frac{\nu}{u_{\min}}}}, & \nu < 0 \end{cases} \tag{5}$$

and $\Delta(\nu) = u(\nu) - h(\nu)$ satisfying $|\Delta(\nu)| \leq \max\{u_{\max}(1 - \tanh(1)), u_{\min}(\tanh(1) - 1)\} = D$. Then, there is a constant $\mu, 0 < \mu < 1$, and one can get $h(\nu) = h_{\nu_\mu} \nu$ when selecting $\nu_0 = 0$. One can get

$$u(\nu) = h_{\nu_\mu} \nu + \Delta(\nu) \tag{6}$$

In this article, the event-triggered adaptive fuzzy finite-time controller for FOSs (1) will be constructed, so that:

(1) output y follows desired $y_r(t)$, and the tracking error $\vartheta_1 = y - y_r(t)$ converges to a small neighborhood of the origin in finite time;
(2) the full-state constraints are satisfied no later than the predetermined finite time;
(3) all the signals in the closed-loop system remain boundedness and the Zeno behavior is avoided to occur.

To complete the control objective, the following assumptions are made.

Assumption 1. *For $\forall k_{c_1} > 0$, there exist positive constants A_0, A_1, and A_2, such that $|y_r| \leq A_0 < k_{c_1}$, $|D^{\alpha} y_r(t)| \leq A_1$, and $|D^{2\alpha} y_r(t)| \leq A_2$. In addition, there exists a compact $\Omega_{y_r} = \left\{ \begin{pmatrix} y_r & D^{\alpha} y_r & D^{2\alpha} y_r \end{pmatrix}^{\mathrm{T}} \middle| y_r^2 + (D^{\alpha} y_r)^2 + (D^{2\alpha} y_r)^2 \leq \delta_{y_r}, \delta_{y_r} > 0 \right\}$, such that $\begin{pmatrix} y_r & D^{\alpha} y_r & D^{2\alpha} y_r \end{pmatrix}^{\mathrm{T}} \in \Omega_{y_r}$.*

Assumption 2. *There exist unknown constants $0 < g_{i\min} \leq g_{i\max}$, such that $0 < g_{i\min} \leq |g_i(\underline{x}_i)| \leq g_{i\max}$, $i = 1, 2, \dots, n$. Without loss of generality, it is further assumed that $0 < g_{i\min} \leq g_i(\underline{x}_i) \leq g_{i\max}$.*

2.2. Necessary Preparations

Lemma 1 ([45])**.** *For $\forall q_1, q_2$ and $\forall s_1, s_2, s_3 > 0$, one can obtain:*

$$|q_1|^{s_1} |q_2|^{s_2} \leq \frac{s_1}{s_1 + s_2} s_3 |q_1|^{s_1+s_2} + \frac{s_2}{s_1 + s_2} s_3^{-\frac{s_1}{s_2}} |q_2|^{s_1+s_2} \tag{7}$$

Lemma 2 ([46,47])**.** *If $\varsigma(t)$ satisfy $|\varsigma(t)| \leq k_{b_0}$ for $\forall k_{b_0} > 0$, one can have*

$$\ln \frac{k_{b_0}^2}{k_{b_0}^2 - \varsigma^2(t)} \leq \frac{\varsigma^2(t)}{k_{b_0}^2 - \varsigma^2(t)} \tag{8}$$

Lemma 3 ([48]). *Let $f(x) \in R$ is an unknown function, then there is FLS and a $\forall\varepsilon > 0$ such that*

$$\sup_{x\in\Omega}\left|f(x) - W^{\mathrm{T}}\Psi(x)\right| < \varepsilon \tag{9}$$

where $\Psi(x) \in R^r$ denotes the basis function vector, and $W \in R^r$ represents the ideal constant weight vector.

Lemma 4 ([49,50]). *Let $x(t) \in R^n$, and $D^\alpha\left(x^T(t)Px(t)\right) \leq 2x^T(t)PD^\alpha(x(t))$ holds for $\forall t \geq t_0$ and $\alpha \in (0,1]$, $P = P^T > 0$.*

Lemma 5 ([51]). *Let $h_1(\cdot), h_2(\cdot) \in R$. Assume that the function $h_1(h_2)$ is convex (i.e., $\partial^2 h_1(h_2)/\partial h_2^2 \geq 0$), then, for $\forall t \geq 0$ and $\alpha \in (0,1]$, inequality $D^\alpha h_1(h_2) \leq \partial h_1(h_2)/\partial h_2 \cdot D^\alpha h_2$ holds.*

Lemma 6 ([52]). *Let $f(t) \in C^1((0,+\infty], R)$, then*

$$D^\alpha f^\beta(t) = \frac{\Gamma(1+\beta)\Gamma(2-\alpha)}{\Gamma(1+\beta-\alpha)} f^{\beta-1}(t) D^\alpha f(t) \tag{10}$$

where $\alpha \in (0,1]$, and $\beta \in [1,\infty)$.

Lemma 7 ([53]). *For $\forall\varepsilon^* > 0$ and $z \in R$, it holds that*

$$|z| - z\tanh\left(\frac{z}{\varepsilon^*}\right) \leq 0.2785\varepsilon^* \tag{11}$$

3. Main Results

3.1. Design of Adaptive Event-Triggered Controller

To adopt the backstepping technology with the DSC technology, the following coordinate transformations are considered:

$$\begin{aligned} &\vartheta_1 = y - y_r(t) \\ &\vartheta_i = x_i - \Upsilon_{i.l} \\ &\zeta_i = \Upsilon_{i.l} - \Upsilon_{i-1} \\ &i = 2,3,\ldots,n \end{aligned} \tag{12}$$

where ϑ_1 is the tracking error, ϑ_i is the dynamic surface error, ζ_i is the filter output error, Υ_{i-1} is the virtual controller, and $\Upsilon_{i.l}$ is the filter output defined as:

$$\begin{aligned} &\kappa_i D^\alpha \Upsilon_{i.l} = -\Upsilon_{i.l} + \Upsilon_{i-1} \\ &\Upsilon_{i.l}(0) = \Upsilon_{i-1}(0), i = 2,3,\ldots,n. \end{aligned} \tag{13}$$

where κ_i is a constant.

For $t \in [t_k, t_{k+1})$, the virtual control laws and actual control law are designed as follows:

$$\begin{aligned} \Upsilon_1 = \frac{1}{g_1(x_1)}\Bigg(&-\frac{c_1\vartheta_1^{2\rho-1}}{\left(k_{b_1}^2-\vartheta_1^2\right)^{\rho-1}} \\ &-\left(\frac{g_{1\min}}{2b_1^2}\theta_1 \parallel \Psi_1(Z_1) \parallel^2 + \frac{1+g_{1\max}^2}{2}d_1^2\right)\frac{\vartheta_1}{k_{b_1}^2-\vartheta_1^2}\Bigg) \end{aligned} \tag{14}$$

$$\begin{aligned} \Upsilon_i = \frac{1}{g_i(\underline{x}_i)}\Bigg(&-\left(\frac{1}{2b_i^2}\theta_i\, g_{i\min} \parallel \Psi_i(\underline{x}_i) \parallel^2 + \frac{1+g_{i\max}^2}{2}d_i^2\right)\frac{\vartheta_i}{k_{b_i}^2-\vartheta_i^2} \\ &+D^\alpha\Upsilon_{i.l} - \frac{c_i\vartheta_i^{2\rho-1}}{\left(k_{b_i}^2-\vartheta_i^2\right)^{\rho-1}} - \frac{g_{i-1}(\underline{x}_{i-1})\vartheta_{i-1}\left(k_{b_i}^2-\vartheta_i^2\right)}{k_{b_{i-1}}^2-\vartheta_{i-1}^2}\Bigg) \\ i = 2,\ldots,&n-1 \end{aligned} \tag{15}$$

$$\begin{aligned} \Upsilon_n = \frac{1}{g_n(x)h_{v_\mu}}\Bigg(&-\left(\frac{1}{2b_n^2}\theta_n\, g_{n\min} \parallel \Psi_n(x) \parallel^2 + \frac{1+g_{n\max}^2}{2}d_n^2\right)\frac{\vartheta_n}{k_{b_n}^2-\vartheta_n^2} \\ &+D^\alpha\Upsilon_{n.l} - \frac{c_n\vartheta_n^{2\rho-1}}{\left(k_{b_n}^2-\vartheta_n^2\right)^{\rho-1}} - \frac{g_{n-1}(\underline{x}_{n-1})\vartheta_{n-1}\left(k_{b_n}^2-\vartheta_n^2\right)}{k_{b_{n-1}}^2-\vartheta_{n-1}^2}\Bigg) \end{aligned} \tag{16}$$

$$\Theta(t) = -(1+\lambda_1^*)\left(\Upsilon_n\tanh\left(\frac{\Upsilon_n\vartheta_n}{\kappa^*\left(k_{b_n}^2-\vartheta_n^2\right)}\right) + \overline{\lambda}_2^*\tanh\left(\frac{\overline{\lambda}_2^*\vartheta_n}{\kappa^*\left(k_{b_n}^2-\vartheta_n^2\right)}\right)\right) \tag{17}$$

$$v(t) = \Theta(t_k), \forall t \in [t_k, t_{k+1}) \tag{18}$$

where t_k is the controller update time, $k \in Z^+$. $b_i, c_i, d_i > 0$ and $\kappa^* > 0$ are the design parameters. $k_{b_i} > 0$ will be given later, $i = 1, 2, \ldots, n$. $\Psi_i(\cdot)$ is the basis function vector and will be specified later, θ_i is the estimate parameter of $\theta_i^* = \frac{1}{g_{i\min}} \| W_i^* \|^2$, and W_i^* is the optimal fuzzy weight in step i. $\overline{\lambda}_2^* > \frac{\lambda_2^*}{1-\lambda_1^*}, \lambda_1^* \in (0,1)$ and $\lambda_2^* > 0$ are the design parameters.

The parameter adaptive laws are designed as follows:

$$D^\alpha \theta_1 = \frac{\gamma_1}{2b_1^2} \frac{\vartheta_1^2}{\left(k_{b_1}^2 - \vartheta_1^2\right)^2} \| \Psi_1(Z_1) \|^2 - \varsigma_1 \theta_1 \tag{19}$$

$$D^\alpha \theta_i = \frac{\gamma_i}{2b_i^2} \frac{\vartheta_i^2}{\left(k_{b_i}^2 - \vartheta_i^2\right)^2} \| \Psi_i(\underline{x}_i) \|^2 - \varsigma_i \theta_i, i = 2, \ldots, n \tag{20}$$

where $\gamma_1 > 0$, $\varsigma_1 > 0$, $\gamma_i > 0$ and $\varsigma_i > 0$ are the design parameters.

The event sampling error is designed as

$$\Upsilon(t) = \Theta(t) - \Theta(t_k), \forall t \in [t_k, t_{k+1}) \tag{21}$$

Then the sampling instants from (18) are determined by the following triggering condition

$$t_{k+1} = \inf\{ t \in R | |\Upsilon(t)| \geq \lambda_1^* |v(t)| + \lambda_2^* \} \tag{22}$$

3.2. Stability Analysis

The details of the proposed control scheme are given by using the backstepping technique, which involves n recursive steps.

Step 1: From (1) and (12), the derivative of ϑ_1 is

$$\begin{aligned} D^\alpha \vartheta_1 &= D^\alpha y - D^\alpha y_r(t) \\ &= f_1(x_1) + g_1(x_1)x_2 - D^\alpha y_r(t) \\ &= W_1^{*\mathrm{T}} \Psi_1(Z_1) + \varepsilon_1 + g_1(x_1)(\vartheta_2 + \zeta_2 + \Upsilon_1) \end{aligned} \tag{23}$$

where $F_1(Z_1) = F_1(x_1, D^\alpha y_r(t)) = f_1(x_1) - D^\alpha y_r(t)$ is approximated via the fuzzy system $W_1^{*\mathrm{T}} \Psi_1(Z_1)$ according to Lemma 3, and satisfies $F_1(Z_1) = W_1^{*\mathrm{T}} \Psi_1(Z_1) + \varepsilon_1$. Assume that there exists $\bar{\varepsilon}_1 > 0$ such that $\varepsilon_1 \leq \bar{\varepsilon}_1$.

Construct the Lyapunov function candidate as

$$V_1 = \frac{1}{2} \ln \frac{k_{b_1}^2}{k_{b_1}^2 - \vartheta_1^2} + \frac{g_{1\min}}{2\gamma_1} \widetilde{\theta}_1^2 \tag{24}$$

where $\widetilde{\theta}_1 = \theta_1^* - \theta_1$.

Based on Lemmas 4 and 5, the αth Caputo fractional derivative of V_1 on each time interval $[t_k, t_{k+1})$ is

$$\begin{aligned} D^\alpha V_1 &= \tfrac{\vartheta_1}{k_{b_1}^2 - \vartheta_1^2} D^\alpha \vartheta_1 - \tfrac{g_{1\min}}{\gamma_1} \widetilde{\theta}_1 D^\alpha \theta_1 \\ &= \tfrac{\vartheta_1}{k_{b_1}^2 - \vartheta_1^2} W_1^{*\mathrm{T}} \Psi_1(Z_1) + \tfrac{\vartheta_1}{k_{b_1}^2 - \vartheta_1^2} (\varepsilon_1 + g_1(x_1)(\vartheta_2 + \zeta_2 + \Upsilon_1)) \\ &- \tfrac{g_{1\min}}{\gamma_1} \widetilde{\theta}_1 D^\alpha \theta_1 \end{aligned} \tag{25}$$

The Young's inequality and Assumption 1 are applied and yields:

$$\frac{\vartheta_1}{k_{b_1}^2 - \vartheta_1^2} W_1^{*\mathrm{T}} \Psi_1(Z_1) \leq \frac{1}{2b_1^2} \frac{\vartheta_1^2}{\left(k_{b_1}^2 - \vartheta_1^2\right)^2} \theta_1^* \, g_{1\min} \| \Psi_1(Z_1) \|^2 + \frac{1}{2} b_1^2 \tag{26}$$

$$\frac{\vartheta_1(\varepsilon_1 + g_1(x_1)\zeta_2)}{k_{b_1}^2 - \vartheta_1^2} \leq \frac{d_1^2 (1 + g_{1\max}^2) \vartheta_1^2}{2\left(k_{b_1}^2 - \vartheta_1^2\right)^2} + \frac{1}{2} d_1^2 \bar{\varepsilon}_1^2 + \frac{1}{2} d_1^2 \zeta_2^2 \tag{27}$$

Substituting (26) and (27) into (25), one can get

$$\begin{aligned}&D^\alpha V \le g_1(x_1)\tfrac{\vartheta_1\vartheta_2}{k_{b_1}^2-\vartheta_1^2} + \tfrac{1}{2}b_1^2 + \tfrac{1}{2}d_1^2\bar{\varepsilon}_1^2 + \tfrac{1}{2}d_1^2\zeta_2^2 \\ &-g_{1\min}\widetilde{\theta}_1\left(\tfrac{1}{\gamma_1}D^\alpha\theta_1 - \tfrac{1}{2b_1^2}\tfrac{\vartheta_1^2}{\left(k_{b_1}^2-\vartheta_1^2\right)^2}\|\ \Psi_1(Z_1)\ \|^2\right) \\ &+\left(\tfrac{g_{1\min}}{2b_1^2}\theta_1\ \|\ \Psi_1(Z_1)\ \|^2 + \tfrac{1+g_{1\max}^2}{2}d_1^2\right)\tfrac{\vartheta_1^2}{\left(k_{b_1}^2-\vartheta_1^2\right)^2} \\ &+g_1(x_1)\Upsilon_1\tfrac{\vartheta_1}{k_{b_1}^2-\vartheta_1^2}\end{aligned} \tag{28}$$

Substituting (14) and (19) into (28), $D^\alpha V_1$ is presented as:

$$\begin{aligned}D^\alpha V_1 \le &-\tfrac{c_1\vartheta_1^{2\rho}}{\left(k_{b_1}^2-\vartheta_1^2\right)^\rho} + g_1(x_1)\tfrac{\vartheta_1\vartheta_2}{k_{b_1}^2-\vartheta_1^2} \\ &+\tfrac{1}{2}b_1^2 + \tfrac{1}{2}d_1^2\bar{\varepsilon}_1^2 + \tfrac{1}{2}d_1^2\zeta_2^2 + \tfrac{g_{1\min}\varsigma_1}{\gamma_1}\widetilde{\theta}_1\theta_1\end{aligned} \tag{29}$$

Step $i(i = 2, 3, \ldots, n-1)$: The derivative of ϑ_i is presented as:

$$\begin{aligned}&D^\alpha\vartheta_i = D^\alpha x_i - D^\alpha\Upsilon_{i.l} \\ &= f_i(\underline{x}_i) + g_i(\underline{x}_i)x_{i+1} - D^\alpha\Upsilon_{i.l} \\ &= W_i^{*\mathrm{T}}\Psi_i(\underline{x}_i) + \varepsilon_i + g_i(\underline{x}_i)(\vartheta_{i+1} + \zeta_{i+1} + \Upsilon_i) - D^\alpha\Upsilon_{i.l}\end{aligned} \tag{30}$$

where $f_i(\underline{x}_i)$ is approximated by $W_i^{*\mathrm{T}}\Psi_i(\underline{x}_i)$ such that $f_i(\underline{x}_i) = W_i^{*\mathrm{T}}\Psi_i(\underline{x}_i) + \varepsilon_i$, and there exists constant $\bar{\varepsilon}_i > 0$ satisfying $\varepsilon_i \le \bar{\varepsilon}_i$.

The Lyapunov candidate function is selected as

$$V_i = V_{i-1} + \frac{1}{2}\ln\frac{k_{b_i}^2}{k_{b_i}^2 - \vartheta_i^2} + \frac{g_{i\min}}{2\gamma_i}\widetilde{\theta}_i^2 + \frac{1}{2}\zeta_i^2 \tag{31}$$

where $\widetilde{\theta}_i = \theta_i^* - \theta_i$ denotes the estimation error.

The αth Caputo fractional derivative of V_i is

$$\begin{aligned}&D^\alpha V_i = D^\alpha V_{i-1} + \tfrac{\vartheta_i}{k_{b_i}^2-\vartheta_i^2}W_i^{*\mathrm{T}}\Psi_i(\underline{x}_i) \\ &+\tfrac{\vartheta_i}{k_{b_i}^2-\vartheta_i^2}(\varepsilon_i + g_i(\underline{x}_i)(\vartheta_{i+1} + \zeta_{i+1} + \Upsilon_i) - D^\alpha\Upsilon_{i.l}) \\ &-\tfrac{g_{i\min}}{\gamma_i}\widetilde{\theta}_i D^\alpha\theta_i + \zeta_i D^\alpha\zeta_i\end{aligned} \tag{32}$$

According to the Young's inequality, the following inequality can be obtained:

$$\frac{\vartheta_i}{k_{b_i}^2 - \vartheta_i^2}W_i^{*\mathrm{T}}\Psi_i(\underline{x}_i) \le \frac{1}{2b_i^2}\frac{\vartheta_i^2}{\left(k_{b_i}^2 - \vartheta_i^2\right)^2}\theta_i^*\ g_{i\min}\|\ \Psi_i(\underline{x}_i)\ \|^2 + \frac{1}{2}b_i^2 \tag{33}$$

$$\frac{\vartheta_i(\varepsilon_i + g_i(\underline{x}_i)\zeta_{i+1})}{k_{b_i}^2 - \vartheta_i^2} \le \frac{d_i^2\left(1 + g_{i\max}^2\right)\vartheta_i^2}{2\left(k_{b_i}^2 - \vartheta_i^2\right)^2} + \frac{1}{2}d_i^2\bar{\varepsilon}_i^2 + \frac{1}{2}d_i^2\zeta_{i+1}^2 \tag{34}$$

Substituting (33) and (34) into (32), yields

$$\begin{aligned}&D^\alpha V_i \le D^\alpha V_{i-1} + \tfrac{1}{2b_i^2}\tfrac{\vartheta_i^2}{\left(k_{b_i}^2-\vartheta_i^2\right)^2}\theta_i^*\ g_{i\min}\|\ \Psi_i(\underline{x}_i)\ \|^2 + \tfrac{1}{2}b_i^2 \\ &-\tfrac{g_{i\min}}{\gamma_i}\widetilde{\theta}_i D^\alpha\theta_i + \zeta_i D^\alpha\zeta_i + \tfrac{\left(1+g_{i\max}^2\right)\vartheta_i^2}{2\left(k_{b_i}^2-\vartheta_i^2\right)^2} + \tfrac{1}{2}d_i^2\bar{\varepsilon}_i^2 + \tfrac{1}{2}d_i^2\zeta_{i+1}^2 \\ &+\tfrac{\vartheta_i}{k_{b_i}^2-\vartheta_i^2}(g_i(\underline{x}_i)(\vartheta_{i+1} + \Upsilon_i) - D^\alpha\Upsilon_{i.l})\end{aligned} \tag{35}$$

Based on Lemma 5, formulas (12), (13), and DSC technology, one can get

$$D^\alpha\zeta_i = D^\alpha\Upsilon_{i.l} - D^\alpha\Upsilon_{i-1} = -\frac{\zeta_i}{\kappa_i} + H_i(\cdot) \tag{36}$$

where

$$H_i(\cdot) = -\sum_{j=1}^{i-1} \frac{\partial \Upsilon_{i-1}}{\partial x_j} D^\alpha x_j - \frac{\partial \Upsilon_{i-1}}{\partial \theta_{i-1}} D^\alpha \theta_{i-1} - \frac{\partial \Upsilon_{i-1}}{\partial \Upsilon_{i-1.l}} D^\alpha \Upsilon_{i-1.l} \tag{37}$$

Substituting (15), (19) and (36) into (35), the $D^\alpha V_i$ can be rewritten as

$$\begin{aligned}
&D^\alpha V_i \le D^\alpha V_{i-1} + \tfrac{g_i(\underline{x}_i)\vartheta_i\vartheta_{i+1}}{k_{b_i}^2-\vartheta_i^2} \\
&-\tfrac{c_i\vartheta_i^{2\rho}}{\left(k_{b_i}^2-\vartheta_i^2\right)^\rho} - \tfrac{g_{i-1}(\underline{x}_{i-1})\vartheta_{i-1}\vartheta_i}{\left(k_{b_{i-1}}^2-\vartheta_{i-1}^2\right)} \\
&+\tfrac{g_{i\min}\varsigma_i}{\gamma_i}\widetilde{\theta}_i\theta_i + \zeta_i D^\alpha\zeta_i + \tfrac{1}{2}d_i^2\bar{\varepsilon}_i^2 + \tfrac{1}{2}d_i^2\zeta_{i+1}^2 + \tfrac{1}{2}b_i^2 \\
&\le -\sum_{j=1}^{i-1}\tfrac{c_j\vartheta_j^{2\rho}}{\left(k_{b_j}^2-\vartheta_j^2\right)^\rho} + \sum_{j=1}^{i-1}\tfrac{g_{j\min}\varsigma_j}{\gamma_j}\widetilde{\theta}_j\theta_j \\
&+\sum_{j=1}^{i-1}\tfrac{1}{2}d_j^2\bar{\varepsilon}_j^2 + \sum_{j=1}^{i-1}\tfrac{1}{2}d_j^2\zeta_{j+1}^2 + \sum_{j=1}^{i-1}\tfrac{1}{2}b_j^2 \\
&+\tfrac{g_{i-1}(\underline{x}_{i-1})\vartheta_{i-1}\vartheta_i}{k_{b_{i-1}}^2-\vartheta_{i-1}^2} + \sum_{j=1}^{i-2}\zeta_{j+1}D^\alpha\zeta_{j+1} \\
&+\tfrac{g_i(\underline{x}_i)\vartheta_i\vartheta_{i+1}}{k_{b_i}^2-\vartheta_i^2} - \tfrac{c_i\vartheta_i^{2\rho}}{\left(k_{b_i}^2-\vartheta_i^2\right)^\rho} - \tfrac{g_{i-1}(\underline{x}_{i-1})\vartheta_{i-1}\vartheta_i}{\left(k_{b_{i-1}}^2-\vartheta_{i-1}^2\right)} \\
&+\tfrac{g_{i\min}\varsigma_i}{\gamma_i}\widetilde{\theta}_i\theta_i + \zeta_i D^\alpha\zeta_i + \tfrac{1}{2}\bar{\varepsilon}_i^2 + \tfrac{1}{2}\zeta_{i+1}^2 + \tfrac{1}{2}b_i^2 \\
&\le -\sum_{j=1}^{i}\tfrac{c_j\vartheta_j^{2\rho}}{\left(k_{b_j}^2-\vartheta_j^2\right)^\rho} + \sum_{j=1}^{i}\tfrac{g_{j\min}\varsigma_j}{\gamma_j}\widetilde{\theta}_j\theta_j \\
&+\sum_{j=1}^{i}\tfrac{1}{2}d_j^2\bar{\varepsilon}_j^2 + \sum_{j=1}^{i}\tfrac{1}{2}d_j^2\zeta_{j+1}^2 + \sum_{j=1}^{i}\tfrac{1}{2}b_j^2 \\
&-\sum_{j=1}^{i-1}\tfrac{\zeta_{j+1}^2}{\kappa_{j+1}} + \sum_{j=1}^{i-1}\left|\zeta_{j+1}H_{j+1}(\cdot)\right| + \tfrac{g_i(\underline{x}_i)\vartheta_i\vartheta_{i+1}}{k_{b_i}^2-\vartheta_i^2}
\end{aligned} \tag{38}$$

Step n: From (6) and (12), one can get

$$\begin{aligned}
&D^\alpha\vartheta_n = D^\alpha x_n - D^\alpha\Upsilon_{n.l} \\
&= f_n(x) + g_n(x)\Big(h_{\nu_\mu}\nu + \Delta(\nu)\Big) - D^\alpha\Upsilon_{n.l} \\
&= W_n^{*\mathrm{T}}\Psi_n(x) + \varepsilon_n + g_n(x)h_{\nu_\mu}\nu + g_n(x)\Delta(\nu) - D^\alpha\Upsilon_{n.l}
\end{aligned} \tag{39}$$

where $f_n(x) = W_n^{*\mathrm{T}}\Psi_n(x) + \varepsilon_n$, and $\varepsilon_n \le \bar{\varepsilon}_n, \bar{\varepsilon}_n > 0$.

The Lyapunov function candidate is as following

$$V_n = V_{n-1} + \frac{1}{2}\ln\frac{k_{b_n}^2}{k_{b_n}^2 - \vartheta_n^2} + \frac{g_{n\min}}{2\gamma_n}\widetilde{\theta}_n^2 + \frac{1}{2}\zeta_n^2 \tag{40}$$

where $\widetilde{\theta}_n = \theta_n^* - \theta_n$.

Then, one can have

$$\begin{aligned}
&D^\alpha V_n = D^\alpha V_{n-1} + \tfrac{\vartheta_n}{k_{b_n}^2-\vartheta_n^2}W_n^{*\mathrm{T}}\Psi_n(x) \\
&+\tfrac{\vartheta_n}{k_{b_n}^2-\vartheta_n^2}\Big(\varepsilon_n + g_n(x)h_{\nu_\mu}\nu + g_n(x)\Delta(\nu) - D^\alpha\Upsilon_{n.l}\Big) \\
&-\tfrac{g_{n\min}}{\gamma_n}\widetilde{\theta}_n D^\alpha\theta_n + \zeta_n D^\alpha\zeta_n
\end{aligned} \tag{41}$$

It is true that

$$\frac{\vartheta_n}{k_{b_n}^2 - \vartheta_n^2}W_n^{*\mathrm{T}}\Psi_n(x) \le \frac{1}{2b_n^2}\frac{\vartheta_n^2}{\left(k_{b_n}^2 - \vartheta_n^2\right)^2}\theta_n^*\, g_{n\min}\|\ \Psi_n(x)\ \|^2 + \frac{1}{2}b_n^2 \tag{42}$$

$$\frac{\vartheta_n(\varepsilon_n + g_n(x)\Delta(\nu))}{k_{b_n}^2 - \vartheta_n^2} \le \frac{d_n^2(1 + g_{n\max}^2)\vartheta_n^2}{2\left(k_{b_n}^2 - \vartheta_n^2\right)^2} + \frac{1}{2}d_n^2\bar{\varepsilon}_n^2 + \frac{1}{2}d_n^2 D^2 \tag{43}$$

and

$$D^\alpha\zeta_n = D^\alpha\Upsilon_{n.l} - D^\alpha\Upsilon_{n-1} = -\frac{\zeta_n}{\kappa_n} + H_n(\cdot) \tag{44}$$

where

$$H_n(\cdot) = -\sum_{j=1}^{n} \frac{\partial \Upsilon_{n-1}}{\partial x_j} D^\alpha x_j - \frac{\partial \Upsilon_{n-1}}{\partial \theta_{n-1}} D^\alpha \theta_{n-1} - \frac{\partial \Upsilon_{n-1}}{\partial \Upsilon_{n-1.l}} D^\alpha \Upsilon_{n-1.l} \tag{45}$$

From Assumption 1 and the boundedness of one V_n are compact, there exists a constant $\Xi_i > 0$, such that $|H_i| \leq \Xi_i$. Then the following inequality holds:

$$|\zeta_i H_i| \leq \frac{\zeta_i^2 \Xi_i^2}{2\widehat{q}_i} + \frac{\widehat{q}_i}{2} \tag{46}$$

where $\widehat{q}_i > 0, i = 1, 2, \ldots, n$.

Substitute (42)–(46), (16) and (20) into (41) yields

$$\begin{aligned}
&D^\alpha V_n \leq D^\alpha V_{n-1} + \tfrac{1}{2b_n^2} \tfrac{\vartheta_n^2}{\left(k_{b_n}^2 - \vartheta_n^2\right)^2} \theta_n^* g_{n\min} \| \Psi_n(x) \|^2 \\
&+ \tfrac{1}{2} b_n^2 + \tfrac{\vartheta_n}{k_{b_n}^2 - \vartheta_n^2} \left(g_n(x) h_{\nu_\mu} \nu - D^\alpha \Upsilon_{n.l} \right) \\
&+ \tfrac{d_n^2 \left(1 + g_{n\max}^2\right) \vartheta_n^2}{2\left(k_{b_n}^2 - \vartheta_n^2\right)^2} + \tfrac{1}{2} d_n^2 \bar{\varepsilon}_n^2 + \tfrac{1}{2} d_n^2 D^2 \\
&- \tfrac{g_{n\min}}{\gamma_n} \widetilde{\theta}_n D^\alpha \theta_n - \tfrac{\zeta_n^2}{\kappa_n} + |\zeta_n H_n(\cdot)| \\
&\leq D^\alpha V_{n-1} - \tfrac{\zeta_n^2}{\kappa_n} + \tfrac{\zeta_n^2 \Xi_n^2}{2\widehat{q}_n} + \tfrac{\widehat{q}_n}{2} + \tfrac{1}{2} d_n^2 \bar{\varepsilon}_n^2 \\
&+ \tfrac{1}{2} d_n^2 D^2 + \tfrac{1}{2} b_n^2 + \tfrac{\vartheta_n}{k_{b_n}^2 - \vartheta_n^2} \left(g_n(x) h_{\nu_\mu} \nu - D^\alpha \Upsilon_{n.l} \right) \\
&+ \left(\tfrac{1}{2b_n^2} \theta_n g_{n\min} \| \Psi_n(x) \|^2 + \tfrac{1 + g_{n\max}^2}{2} d_n^2 \right) \tfrac{\vartheta_n^2}{\left(k_{b_n}^2 - \vartheta_n^2\right)^2} \\
&- \tfrac{g_{n\min}}{\gamma_n} \widetilde{\theta}_n \left(D^\alpha \theta_n - \tfrac{\gamma_n}{2b_n^2} \tfrac{\vartheta_n^2}{\left(k_{b_n}^2 - \vartheta_n^2\right)^2} \| \Psi_n(x) \|^2 \right)
\end{aligned} \tag{47}$$

Theorem 1. *Consider the nonlinear FOSs (1) with the Assumptions 1 and 2. If the initial conditions satisfy $x_i(0) \in \Omega_x = \{ x_i | |x_i(0)| < k_{c_i} \}$, the actual controller (18) with virtual controllers (14)–(16), and parameter adaptive laws (19) and (20) can confirm that all the signals in the closed-loop system are bounded, all the states $x(t)$ do not transgress the pregiven sets, and the Zeno behavior is excluded. Moreover, for $\forall t \geq T$, the closed-loop error signal ϑ_i will stay around the compact set*

$$\Omega_{\vartheta_i} = \left\{ \vartheta_i | |\vartheta_i| \leq k_{b_i} \sqrt{1 - e^{-2(\mathrm{M}/(\sigma(1-\vartheta)))^{1/\rho}}} \right\}, i = 1, 2, \ldots, n \tag{48}$$

where

$$\begin{aligned}
T &= \left(\tfrac{\Gamma\left(\frac{2-\rho}{1-\rho}\right) \Gamma(2-\alpha) \Gamma(\alpha+1)}{\sigma \vartheta \Gamma\left(\frac{2-\rho}{1-\rho} - \alpha\right)} \left(V_n^{1-\rho}(0) - \left(\tfrac{\mathrm{M}}{\sigma(1-\vartheta)} \right)^{\frac{1}{\rho}} \right) \right)^{\frac{1}{\alpha}} \\
&\vartheta \in (0, 1)
\end{aligned} \tag{49}$$

Proof. From the definition $\Delta(t) = \Theta(t) - u(t)$ and (22), one can have

$$\Theta(t) = (1 + \lambda_1^* \lambda_1(t)) u(t) + \lambda_2^* \lambda_2(t) \tag{50}$$

where $|\lambda_1(t)| \leq 1$ and $|\lambda_2(t)| \leq 1$. Accordingly, one can obtain

$$\nu(t) = \frac{\Theta(t) - \lambda_2^* \lambda_2(t)}{1 + \lambda_1^* \lambda_1(t)} \tag{51}$$

According to (16), (18), (19) and (51), inequality (47) can be rewritten as

$$\begin{aligned}
&D^\alpha V_n \leq D^\alpha V_{n-1} + \tfrac{g_n(x) h_{\nu_\mu} \vartheta_n}{k_{b_n}^2 - \vartheta_n^2} \tfrac{\Theta(t) - \lambda_2^* \lambda_2(t)}{1 + \lambda_1^* \lambda_1(t)} \\
&- \tfrac{c_n \vartheta_n^{2\rho}}{\left(k_{b_n}^2 - \vartheta_n^2\right)^\rho} - \tfrac{g_{n-1}(\underline{x}_{n-1}) \vartheta_{n-1} \vartheta_n}{k_{b_{n-1}}^2 - \vartheta_{n-1}^2} \\
&- g_n(x) h_{\nu_\mu} \tfrac{\Upsilon_n \vartheta_n}{k_{b_n}^2 - \vartheta_n^2} + \tfrac{g_{n\min}}{\gamma_n} \varsigma_n \widetilde{\theta}_n \theta_n \\
&- \tfrac{\zeta_n^2}{\kappa_n} + \tfrac{\zeta_n^2 \Xi_n^2}{2\widehat{q}_n} + \tfrac{\widehat{q}_n}{2} + \tfrac{1}{2} d_n^2 \bar{\varepsilon}_n^2 + \tfrac{1}{2} d_n^2 D^2 + \tfrac{1}{2} b_n^2
\end{aligned} \tag{52}$$

In view of $|\lambda_1(t)| \leq 1$ and $|\lambda_2(t)| \leq 1$, one can have

$$\begin{aligned} \frac{\Theta(t)\vartheta_n}{1+\lambda_1^*\lambda_1(t)} &\leq \frac{\Theta(t)\vartheta_n}{1+\lambda_1^*} \\ \frac{\lambda_2^*\lambda_2(t)}{1+\lambda_1^*\lambda_1(t)} &\leq \left|\frac{\lambda_2^*}{1-\lambda_1^*}\right| \end{aligned} \tag{53}$$

Using Lemma 7, it follows that

$$\begin{aligned} & D^\alpha V_n \leqslant D^\alpha V_{n-1} + \tfrac{g_{n\min}}{\gamma_n}\varsigma_n\widetilde{\theta}_n\theta_n - \tfrac{c_n\vartheta_n^{2\rho}}{\left(k_{b_n}^2-\vartheta_n^2\right)^\rho} \\ & -\tfrac{g_n(x)h_{\nu_\mu}\Upsilon_n\vartheta_n}{k_{b_n}^2-\vartheta_n^2} - \tfrac{\Upsilon_n\vartheta_n g_n(x)}{k_{b_n}^2-\vartheta_n^2}\tanh\left(\tfrac{\Upsilon_n\vartheta_n}{\kappa^*\left(k_{b_n}^2-\vartheta_n^2\right)}\right) \\ & -\tfrac{g_n(x)h_{\nu_\mu}\vartheta_n}{k_{b_n}^2-\vartheta_n^2}\tfrac{\lambda_2^*\lambda_2(t)}{1+\lambda_1^*\lambda_1(t)} + \tfrac{\overline{\lambda}_2^*\vartheta_n g_n(x)}{k_{b_n}^2-\vartheta_n^2}\tanh\left(\tfrac{\overline{\lambda}_2^*\vartheta_n}{\kappa^*\left(k_{b_n}^2-\vartheta_n^2\right)}\right) \\ & -\tfrac{g_{n-1}\left(\underline{x}_{n-1}\right)\vartheta_{n-1}\vartheta_n}{k_{b_{n-1}}^2-\vartheta_{n-1}^2} - \tfrac{\zeta_n^2}{\kappa_n} + \tfrac{\zeta_n^2\Xi_n^2}{2\widehat{q}_n} + \tfrac{\widehat{q}_n}{2} + \tfrac{1}{2}d_n^2\bar{\varepsilon}_n^2 + \tfrac{1}{2}d_n^2D^2 + \tfrac{1}{2}b_n^2 \\ & \leqslant D^\alpha V_{n-1} + \tfrac{g_{n\min}}{\gamma_n}\varsigma_n\widetilde{\theta}_n\theta_n - \tfrac{c_n\vartheta_n^{2\rho}}{\left(k_{b_n}^2-\vartheta_n^2\right)^\rho} \\ & +h_{\nu_\mu}g_n(x)\left(\left|\tfrac{\overline{\lambda}_2^*\vartheta_n}{k_{b_n}^2-\vartheta_n^2}\right| - \tfrac{\overline{\lambda}_2^*\vartheta_n}{k_{b_n}^2-\vartheta_n^2}\tanh\left(\tfrac{\overline{\lambda}_2^*\vartheta_n}{\kappa^*\left(k_{b_n}^2-\vartheta_n^2\right)}\right)\right) \\ & +h_{\nu_\mu}g_n(x)\left(\left|\tfrac{\Upsilon_n\vartheta_n}{k_{b_n}^2-\vartheta_n^2}\right| - \tfrac{\Upsilon_n\vartheta_n}{k_{b_n}^2-\vartheta_n^2}\tanh\left(\tfrac{\Upsilon_n\vartheta_n}{\kappa^*\left(k_{b_n}^2-\vartheta_n^2\right)}\right)\right) \\ & -\tfrac{g_{n-1}\left(\underline{x}_{n-1}\right)\vartheta_{n-1}\vartheta_n}{k_{b_{n-1}}^2-\vartheta_{n-1}^2} - \tfrac{\zeta_n^2}{\kappa_n} + \tfrac{\zeta_n^2\Xi_n^2}{2\widehat{q}_n} + \tfrac{\widehat{q}_n}{2} + \tfrac{1}{2}d_n^2\bar{\varepsilon}_n^2 + \tfrac{1}{2}d_n^2D^2 + \tfrac{1}{2}b_n^2 \\ & \leqslant D^\alpha V_{n-1} - \tfrac{c_n\vartheta_n^{2\rho}}{\left(k_{b_n}^2-\vartheta_n^2\right)^\rho} - \tfrac{g_{n-1}\left(\underline{x}_{n-1}\right)\vartheta_{n-1}\vartheta_n}{k_{b_{n-1}}^2-\vartheta_{n-1}^2} - \tfrac{g_{n\min}}{\gamma_n}\varsigma_n\widetilde{\theta}_n\theta_n \\ & -\tfrac{\zeta_n^2}{\kappa_n} + \tfrac{\zeta_n^2\Xi_n^2}{2\widehat{q}_n} + \tfrac{\widehat{q}_n}{2} + \tfrac{1}{2}d_n^2\bar{\varepsilon}_n^2 + \tfrac{1}{2}d_n^2D^2 + \tfrac{1}{2}b_n^2 + 0.557\kappa^* g_{n\max}h_{\nu_\mu} \\ & \leqslant -\sum_{j=1}^{n}\tfrac{c_j\vartheta_j^{2\rho}}{\left(k_{b_j}^2-\vartheta_j^2\right)^\rho} + \sum_{j=1}^{n}\tfrac{g_{j\min}\varsigma_j}{\gamma_j}\widetilde{\theta}_j\theta_j \\ & +\sum_{j=1}^{n-1}\tfrac{1}{2}d_j^2\zeta_{j+1}^2 - \sum_{j=1}^{n-1}\tfrac{\zeta_{j+1}^2}{\kappa_{j+1}} + \sum_{j=1}^{n-1}\tfrac{\zeta_{j+1}^2\Xi_{j+1}^2}{2\widehat{q}_{j+1}} + \sum_{j=1}^{n-1}\tfrac{\widehat{q}_{j+1}}{2} \\ & +\sum_{j=1}^{n}\tfrac{1}{2}d_j^2\bar{\varepsilon}_j^2 + \sum_{j=1}^{n}\tfrac{1}{2}b_j^2 + \tfrac{1}{2}d_n^2D^2 + 0.557\kappa^* g_{n\max}h_{\nu_\mu} \end{aligned} \tag{54}$$

Based on the estimation error $\widetilde{\theta}_j = \theta_j^* - \theta_j$, the following inequality holds:

$$\widetilde{\theta}_j\theta_j \leq \frac{1}{2}\theta_j^{*2} - \frac{1}{2}\widetilde{\theta}_j^2 \tag{55}$$

Then, one can obtain

$$\sum_{j=1}^{n}\frac{g_{j\min}\varsigma_j}{\gamma_j}\widetilde{\theta}_j\theta_j \leq \sum_{j=1}^{n}\frac{g_{j\min}\varsigma_j}{2\gamma_j}\theta_i^{*2} - \sum_{j=1}^{n}\frac{g_{j\min}\varsigma_j}{2\gamma_j}\widetilde{\theta}_i^2 \tag{56}$$

From (56), (**??**) can be rewritten as

$$\begin{aligned} & D^\alpha V_n \leq -\sum_{j=1}^{n}\tfrac{c_j\vartheta_j^{2\rho}}{\left(k_{b_j}^2-\vartheta_j^2\right)^\rho} + \sum_{j=1}^{n}\tfrac{g_{j\min}\varsigma_j}{2\gamma_j}\theta_i^{*2} - \sum_{j=1}^{n}\tfrac{g_{j\min}\varsigma_j}{2\gamma_j}\widetilde{\theta}_i^2 \\ & +\sum_{j=1}^{n}\tfrac{1}{2}d_j^2\bar{\varepsilon}_j^2 + \sum_{j=1}^{n-1}\tfrac{1}{2}d_j^2\zeta_{j+1}^2 - \sum_{j=1}^{n-1}\tfrac{\zeta_{j+1}^2}{\kappa_{j+1}} + \sum_{j=1}^{n-1}\tfrac{\zeta_{j+1}^2\Xi_{j+1}^2}{2\widehat{q}_{j+1}} + \sum_{j=1}^{n-1}\tfrac{\widehat{q}_{j+1}}{2} \\ & +\sum_{j=1}^{n}\tfrac{1}{2}b_j^2 + \tfrac{1}{2}d_n^2D^2 + 0.557\kappa^* g_{n\max}h_{\nu_\mu} \\ & \leq -\sigma\left(\sum_{j=1}^{n}\left(\tfrac{\vartheta_j^2}{2\left(k_{b_j}^2-\vartheta_j^2\right)}\right)^\rho + \sum_{j=1}^{n}\tfrac{g_{j\min}}{2\gamma_j}\widetilde{\theta}_i^2 + \sum_{j=1}^{n-1}\tfrac{1}{2}\zeta_{j+1}^2\right) + \Theta \end{aligned} \tag{57}$$

where

$$\begin{aligned}
&\sigma = \min\left\{2^{\rho}c_i, \varsigma_i, \tfrac{2}{\kappa_{j+1}} - d_j^2 - \tfrac{\Xi_{j+1}^2}{\widehat{q}_{j+1}}, i = 1, \ldots, n; j = 1, \ldots, n-1\right\} \\
&\Theta = \sum_{j=1}^{n} \tfrac{1}{2}d_j^2\bar{\varepsilon}_j^2 + \sum_{j=1}^{n} \tfrac{1}{2}b_j^2 + \tfrac{1}{2}d_n^2 D^2 + \sum_{j=1}^{n} \tfrac{g_{j\min}\varsigma_j}{2\gamma_j}\theta_j^{*2} + \sum_{j=1}^{n-1} \tfrac{\widehat{q}_{j+1}}{2} \\
&\quad +0.557\kappa^* g_{n\max} h_{\nu_\mu}
\end{aligned} \tag{58}$$

According to Lemma 1, choose $q_1 = 1, q_2 = \sum_{j=1}^{n} \frac{g_{j\min}}{2\gamma_j}\tilde{\theta}_j^2, s_1 = 1-\rho, s_2 = \rho$ and $s_3 = \rho^{\frac{\rho}{1-\rho}}$, then one can obtain

$$\left(\sum_{j=1}^{n} \frac{g_{j\min}}{2\gamma_j}\tilde{\theta}_j^2\right)^{\rho} \le (1-\rho)s_3 + \sum_{j=1}^{n} \frac{g_{j\min}}{2\gamma_j}\tilde{\theta}_j^2 \tag{59}$$

$$\left(\sum_{j=1}^{n-1} \frac{1}{2}\zeta_{j+1}^2\right)^{\rho} \le (1-\rho)s_3 + \sum_{j=1}^{n-1} \frac{1}{2}\zeta_{j+1}^2 \tag{60}$$

Based on (59) and (60), (57) can be rewritten as

$$\begin{aligned}
D^{\alpha}V_n \le &-\sigma\sum_{j=1}^{n}\left(\frac{\vartheta_j^2}{2\left(k_{b_j}^2 - \vartheta_j^2\right)}\right)^{\rho} \\
&-\sigma\left(\sum_{j=1}^{n} \frac{g_{j\min}}{2\gamma_j}\tilde{\theta}_j^2\right)^{\rho} - \sigma\left(\sum_{j=1}^{n-1} \frac{1}{2}\zeta_{j+1}^2\right)^{\rho} + \mathrm{M}
\end{aligned} \tag{61}$$

where $\mathrm{M} = 2\sigma(1-\rho)s_3 + \Theta$.

From Lemma 2, (61) can be described as

$$D^{\alpha}V_n \le -\sigma V_n^{\rho} + \mathrm{M} \tag{62}$$

For $\forall\vartheta \in (0,1)$, (2) can be rewritten as $D^{\alpha}V_n \le -\sigma\vartheta V_n^{\rho} - \sigma(1-\vartheta)V_n^{\rho} + \mathrm{M}$. If $V_n > (\mathrm{M}/(\sigma(1-\vartheta)))^{\frac{1}{\rho}}$, one can obtain

$$D^{\alpha}V_n \le -\sigma\vartheta V_n^{\rho} \tag{63}$$

Let $V = V_n^{1-\rho}$, then $D^{\alpha}V^{\frac{1}{1-\rho}} \le -\sigma\vartheta V^{\frac{\rho}{1-\rho}}$. From Lemma 6, one can get

$$D^{\alpha}V^{\frac{1}{1-\rho}} = \frac{\Gamma\left(\frac{2-\rho}{1-\rho}\right)\Gamma(2-\alpha)}{\Gamma\left(\frac{2-\rho}{1-\rho} - \alpha\right)} V^{\frac{\rho}{1-\rho}} D^{\alpha}V \tag{64}$$

Then

$$D^{\alpha}V \le -\sigma\vartheta\frac{\Gamma\left(\frac{2-\rho}{1-\rho} - \alpha\right)}{\Gamma\left(\frac{2-\rho}{1-\rho}\right)\Gamma(2-\alpha)} \tag{65}$$

From $V = V_n^{1-\rho}$, one get

$$V_n^{1-\rho}(t) - V_n^{1-\rho}(0) \le -\sigma\vartheta\frac{\Gamma\left(\frac{2-\rho}{1-\rho} - \alpha\right)}{\Gamma\left(\frac{2-\rho}{1-\rho}\right)\Gamma(2-\alpha)}\frac{t^{\alpha}}{\Gamma(\alpha+1)} \tag{66}$$

From (66), the finite time T can be designed as (49), and one can get

$$V_n \le (\mathrm{M}/(\sigma(1-\vartheta)))^{\frac{1}{\rho}}, \forall t \ge T \tag{67}$$

Furthermore, based on the definition of V_n, one can obtain

$$\frac{1}{2}\ln\frac{k_{b_i}^2}{k_{b_i}^2 - \vartheta_i^2} \le (\mathrm{M}/(\sigma(1-\vartheta)))^{\frac{1}{\rho}}, \forall t \ge T \tag{68}$$

This implies that

$$|\vartheta_i| \le k_{b_i}\sqrt{1 - e^{-2(\mathrm{M}/(\sigma(1-\vartheta)))^{1/\rho}}}, \forall t \ge T \tag{69}$$

Then, after the finite time T, the tracking error converges to Ω_{ϑ_i}.

The boundedness of $\ln \frac{k_{b_k}^2}{k_{b_i}^2-\vartheta_i^2}$ can be obtained according to (67), thus $|\vartheta_i|$ remains in the set $|\vartheta_i| < k_{b_i}$. Also, it holds that $\widetilde{\theta}_i$ and ζ_{i+1} are bounded. As ϑ_1 and $y_r(t)$ are bounded, then x_1 is bounded. From (14), Υ_1 is a function of ϑ_1 and θ_1. Then, Υ_1 is bounded and satisfies $|\Upsilon_1| < \overline{\Upsilon}_1, \overline{\Upsilon}_1 > 0$. Using $\vartheta_2 = x_2 - \Upsilon_{2.l}$ and $\zeta_2 = \Upsilon_{2.l} - \Upsilon_1$, one can get that $\Upsilon_{2.l}$ and x_2 are bounded. Similarly, the boundedness of states $x_i, i = 3, \ldots, n$, virtual controllers $\Upsilon_i, i = 2, \ldots, n-1$, and controller ν are all obtained. From $x_1 = \vartheta_1 + y_r(t)$ and $|y_r(t)| \leq A_0$ according to Assumption 1, one can have $|x_1| \leq |\vartheta_1| + |y_r(t)| < k_{b_1} + A_0$. Define $k_{b_1} = k_{c_1} - A_0$, one obtain $|\zeta_2| \leq \sqrt{2}(\mathrm{M}/(\sigma(1-\vartheta))(\sigma(1-\vartheta)))^{\frac{1}{2\rho}} = \Delta_2$, for $\forall t \geq T$, yielding $|x_2| \leq |\vartheta_2| + |\zeta_2| + |a_1| < k_{b_2} + \Delta_2 + \overline{a}_1$. Let $k_{b_2} = k_{c_2} - \Delta_2 - \overline{a}_1$, one can get $|x_2| < k_{c_2}$. Similarly, one can in turn obtain $|x_i| < k_{c_i}, i = 3, \ldots, n$. Thus, the condition of the full-state constraints is accomplished.

Now we will show that the proposed strategy can avoid the Zeno behavior, i.e., one can always find a positive $a^* > 0$ such that $t_{k+1} - t_k \geq a^*, \forall k \in Z^+$. From the sampling error (21), one can get $D^\alpha|\Upsilon(t)| = sign(\Upsilon(t))D^\alpha\Upsilon(t) \leq |D^\alpha\Theta(t)|$. Due to (17), $D^\alpha\Theta(t)$ is bounded and $\exists\zeta > 0$ satisfying $|D^\alpha\Theta(t)| < \zeta$. According to $\Upsilon(t_k) = 0$ and $\lim\limits_{t\to t_{k+1}} \Upsilon(t) = \lambda_2^*$, one gets $t_{k+1} - t_k \geq \frac{\lambda_2^*}{\zeta}$, which avoids the Zeno phenomenon. This completes the proof. □

4. Simulation

Consider the following nonlinear FOSs:

$$\begin{cases} D^{0.8}x_1 = 0.8x_1^2 + (6 + 3\sin(x_1))x_2 \\ D^{0.8}x_2 = 0.5x_1^3\cos(x_2) \\ \qquad\qquad + \left(5 + \sin\left(x_1^2\right) + \cos\left(x_1 x_2^2\right)\right)u(v) \end{cases} \tag{70}$$

where $f_1(x_1) = 0.8x_1^2$ and $f_2(x_2) = 0.5x_1^3\cos(x_2)$ are the unknown function, $g_1(x_1) = 6 + 3\sin(x_1)$ and $g_2(x_2) = 5 + \sin\left(x_1^2\right) + \cos\left(x_1 x_2^2\right)$ are the known function. The saturation parameters are $u_{\max} = 0.15$ and $u_{\min} = -0.13$. The state constraints are given as $k_{c_1} = 0.9$ and $k_{c_2} = 0.65$. The reference signal is chosen as $y_r(t) = 0.8\sin(t)$.

The parameters are given as $b_1 = b_2 = 0.1, c_1 = 1, c_2 = 0.8, d_1 = 1, d_2 = 0.5, \kappa_2 = 0.01, \kappa^* = 1.1, \rho = 0.5, \gamma_1 = 6, \gamma_2 = 0.05, \varsigma_1 = 0.1, \varsigma_2 = 0.01, \lambda_1^* = 0.001$ and $\lambda_2^* = 0.1$. The initial values are chosen as $x_1(0) = x_2(0) = 0, \theta_1(0) = 0$ and $\theta_2(0) = 0$.

To deal with the unknown nonlinear $f_1(x_1) = 0.8x_1^2$ and $f_2(x_2) = 0.5x_1^3\cos(x_2)$, the membership functions of FLS are designed as follows:

$$\begin{aligned} &\Psi(x_1) = \exp\left(-\frac{\left(x_1 - x_{k_1}\right)^2}{\delta_1^2}\right) \\ &\Psi(\overline{x}_2) = \exp\left(-\frac{\left(x_1 - x_{k_1}\right)^2}{\delta_1^2} - \frac{\left(x_2 - x_{k_2}\right)^2}{\delta_2^2}\right) \\ &x_{k_1} \in \{0.2k_1 - 1 | k_1 = 1, 2, \ldots, 9\} \\ &x_{k_2} \in \{0.25k_2 - 1 | k_2 = 1, 2, \ldots, 6\} \\ &\delta_1 = 0.15, \delta_2 = 0.15 \end{aligned} \tag{71}$$

Figures 1–6 show the simulation results by the proposed finite-time ECT controller. The trajectories of the tracking error and the system state are shown in Figures 1 and 2. It can be found that the transient response of output y is reasonable in both magnitude and frequency content, state x_1 satisfies $|x_1| \leqslant k_{c_1}$=0.9 and state x_2 satisfies $|x_2| \leqslant k_{c_2}$=0.65, which are not to violate their constraint bound. Figure 3 illustrates the trajectories of parameters estimation, and the controller input u is depicted in Figure 4, which are all bounded. Figures 5 and 6 list the sequence of steps of event-triggered sampling and the number of accumulated events. It demonstrates that the frequency of event-driven controller is not fixed, which is determined by the state error and can save communication resources and computing resources. It is clear that the tracking objective and stability of the closed-loop system in finite time can be achieved, and the communication burden can be reduced effectively.

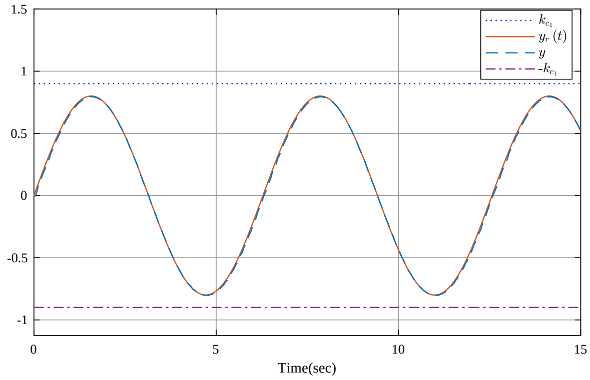

Figure 1. Output y and tracking signal $y_r(t)$.

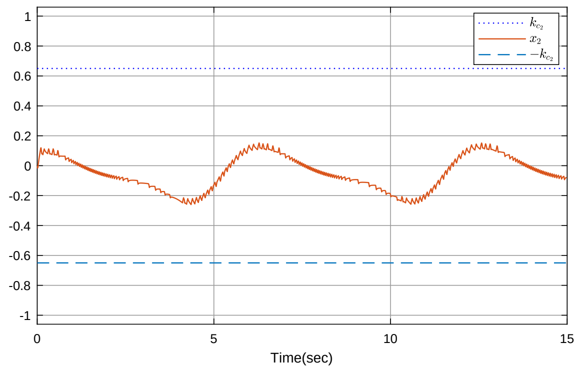

Figure 2. State x_2.

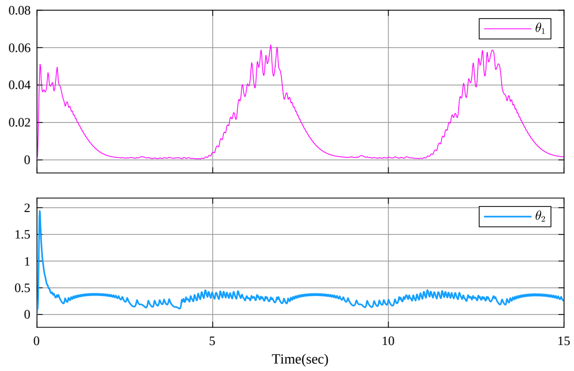

Figure 3. Parameters estimation θ_1 and θ_2.

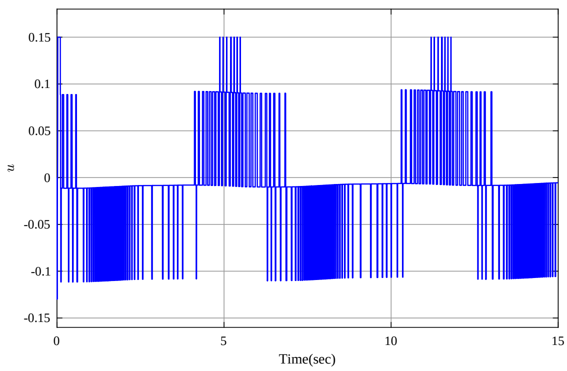

Figure 4. Control input u.

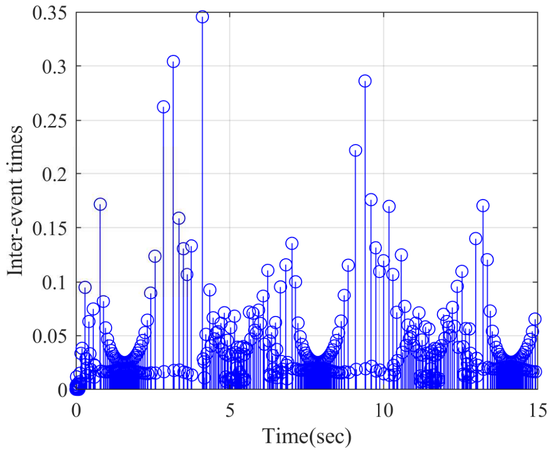

Figure 5. Time interval.

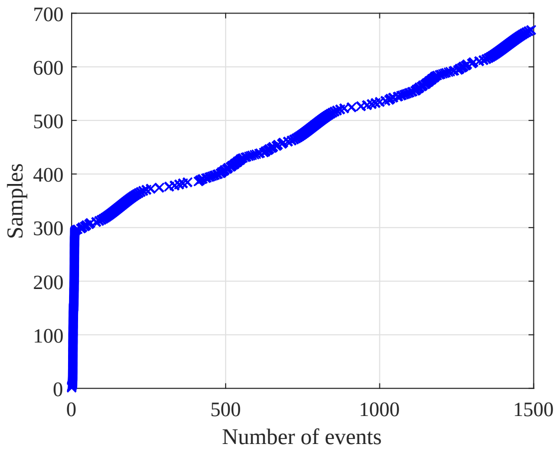

Figure 6. Cumulative number of events.

5. Conclusions

An event-triggered adaptive fuzzy finite-time DSC approach for strict-feedback uncertain nonlinear FOSs with actuator saturation and full-state constraints has been proposed. The dynamic surface method is applied to overcome the difficulty of inherent computational complexity. By employing the BLFs and fractional-order Lyapunov method, the constraints are not violated, the closed-loop system is bounded, and the tracking error converges to a small region around the origin in finite time. Meanwhile, the Zeno behavior can be avoided and the simulation results verify the effectiveness. In the future, we will extend the results of this paper to switched fractional-order nonlinear systems, and apply the theoretical results to practical engineering applications.

Author Contributions: Methodology, C.W.; Software, W.L.; Formal analysis, W.L.; Investigation, C.W. and W.L.; Resources, M.L.; Data curation, M.L.; Writing–original draft, C.W.; Writing–review and editing, M.L. All authors have read and agreed to the published version of the manuscript.

Funding: This paper was supported in part by National Natural Science Foundation of China (62205280).

Data Availability Statement: Data are contained within the article.

Conflicts of Interest: The authors declare no conflict of interest.

References

1. Sun, H.; Zhang, Y.; Baleanu, D.; Chen, W.; Chen, Y. A new collection of real world applications of fractional calculus in science and engineering. *Commun. Nonlinear Sci. Numer. Simul.* **2018**, *64*, 213–231. [CrossRef]
2. Li, Y.; Chen, Y.; Podlubny, I. Mittag–Leffler stability of fractional order nonlinear dynamic systems. *Automatica* **2009**, *45*, 1965–1969. [CrossRef]

3. Soleimanizadeh, A.; Nekoui, M.A. Optimal type-2 fuzzy synchronization of two different fractional-order chaotic systems with variable orders with an application to secure communication. *Soft Comput.* **2021**, *25*, 6415–6426. [CrossRef]
4. Li, R.G.; Wu, H.N. Adaptive synchronization control with optimization policy for fractional-order chaotic systems between 0 and 1 and its application in secret communication. *ISA Trans.* **2019**, *92*, 35–48. [CrossRef] [PubMed]
5. Nguyen, S.D.; Lam, B.D.; Choi, S.B. Smart dampers-based vibration control–Part 2: Fractional-order sliding control for vehicle suspension system. *Mech. Syst. Signal Process.* **2021**, *148*, 107145. [CrossRef]
6. Chen, E.; Xing, W.; Wang, M.; Ma, W.; Chang, Y. Study on chaos of nonlinear suspension system with fractional-order derivative under random excitation. *Chaos Solitons Fractals* **2021**, *152*, 111300. [CrossRef]
7. Jin, T.; Xia, H.; Deng, W.; Li, Y.; Chen, H. Uncertain fractional-order multi-objective optimization based on reliability analysis and application to fractional-order circuit with caputo type. *Circuits Syst. Signal Process.* **2021**, *40*, 5955–5982. [CrossRef]
8. Wang, M.; Liao, X.; Deng, Y.; Li, Z.; Su, Y.; Zeng, Y. Dynamics, synchronization and circuit implementation of a simple fractional-order chaotic system with hidden attractors. *Chaos Solitons Fractals* **2020**, *130*, 109406. [CrossRef]
9. Shi, J.; He, K.; Fang, H. Chaos, Hopf bifurcation and control of a fractional-order delay financial system. *Math. Comput. Simul.* **2022**, *194*, 348–364. [CrossRef]
10. Wang, Y.L.; Jahanshahi, H.; Bekiros, S.; Bezzina, F.; Chu, Y.M.; Aly, A.A. Deep recurrent neural networks with finite-time terminal sliding mode control for a chaotic fractional-order financial system with market confidence. *Chaos Solitons Fractals* **2021**, *146*, 110881. [CrossRef]
11. Yang, B.; Shi, X.; Chen, X. Image Analysis by Fractional-Order Gaussian-Hermite Moments. *IEEE Trans. Image Process.* **2022**, *31*, 2488–2502. [CrossRef] [PubMed]
12. Li, X.; Mou, J.; Xiong, L.; Wang, Z.; Xu, J. Fractional-order double-ring erbium-doped fiber laser chaotic system and its application on image encryption. *Opt. Laser Technol.* **2021**, *140*, 107074. [CrossRef]
13. Gokulakrishnan, V.; Srinivasan, R. *Event-Triggered Controller on Practically Exponential Input-to-State Stabilization of Stochastic Reaction-Diffusion Neural Networks and Its Application to Image Encryption*; Springer: Berlin/Heidelberg, Germany, 2023.
14. Mirzajani, S.; Aghababa, M.P.; Heydari, A. Adaptive T–S fuzzy control design for fractional-order systems with parametric uncertainty and input constraint. *Fuzzy Sets Syst.* **2018**, *365*, 22–39. [CrossRef]
15. Liu, H.; Li, S.; Wang, H.; Sun, Y. Adaptive fuzzy control for a class of unknown fractional-order neural networks subject to input nonlinearities and dead-zones. *Inf. Sci.* **2018**, *454–455*, 30–45. [CrossRef]
16. Song, S.; Park, J.H.; Zhang, B.; Song, X.; Zhang, Z. Adaptive Command Filtered Neuro-Fuzzy Control Design for Fractional-Order Nonlinear Systems with Unknown Control Directions and Input Quantization. *IEEE Trans. Syst. Man Cybern. Syst.* **2020**, *51*, 7238–7249. [CrossRef]
17. Hu, T.; He, Z.; Zhang, X.; Zhong, S. Event-triggered consensus strategy for uncertain topological fractional-order multiagent systems based on Takagi–Sugeno fuzzy models. *Inf. Sci.* **2021**, *551*, 304–323. [CrossRef]
18. Fei, J.; Wang, H.; Fang, Y. Novel neural network fractional-order sliding-mode control with application to active power filter. *IEEE Trans. Syst. Man Cybern. Syst.* **2021**, *52*, 3508–3518. [CrossRef]
19. Gokulakrishnan, V.; Srinivasan, R.; Syed Ali, M.; Rajchakit, G.; Thakur, G. Novel LMI-based adaptive boundary synchronisation of fractional-order fuzzy reaction–diffusion BAM neural networks with leakage delay. *Int. J. Syst. Sci.* **2023**, *54*, 2975–2998. [CrossRef]
20. Liu, H.; Pan, Y.; Cao, J.; Wang, H.; Zhou, Y. Adaptive neural network backstepping control of fractional-order nonlinear systems with actuator faults. *IEEE Trans. Neural Netw. Learn. Syst.* **2020**, *31*, 5166–5177. [CrossRef]
21. Zhan, Y.; Tong, S. Adaptive fuzzy output-feedback decentralized control for fractional-order nonlinear large-scale systems. *IEEE Trans. Cybern.* **2021**, *52*, 12795–12804. [CrossRef]
22. Liu, H.; Pan, Y.; Cao, J. Composite learning adaptive dynamic surface control of fractional-order nonlinear systems. *IEEE Trans. Cybern.* **2019**, *50*, 2557–2567. [CrossRef] [PubMed]
23. Wang, C.; Cui, L.; Liang, M.; Li, J.; Wang, Y. Adaptive Neural Network Control for a Class of Fractional-Order Nonstrict-Feedback Nonlinear Systems with Full-State Constraints and Input Saturation. *IEEE Trans. Neural Netw. Learn. Syst.* **2021**, *33*, 6677–6689. [CrossRef] [PubMed]
24. Shahvali, M.; Azarbahram, A.; Naghibi-Sistani, M.B.; Askari, J. Bipartite consensus control for fractional-order nonlinear multi-agent systems: An output constraint approach. *Neurocomputing* **2020**, *397*, 212–223. [CrossRef]
25. Zouari, F.; Ibeas, A.; Boulkroune, A.; Jinde, C.; Arefi, M.M. Neural network controller design for fractional-order systems with input nonlinearities and asymmetric time-varying Pseudo-state constraints. *Chaos Solitons Fractals* **2021**, *144*, 110742. [CrossRef]
26. Zouari, F.; Ibeas, A.; Boulkroune, A.; Cao, J.; Arefi, M.M. Adaptive neural output-feedback control for nonstrict-feedback time-delay fractional-order systems with output constraints and actuator nonlinearities. *Neural Networks* **2018**, *105*, 256–276. [CrossRef]
27. Wei, M.; Li, Y.X.; Tong, S. Event-triggered adaptive neural control of fractional-order nonlinear systems with full-state constraints. *Neurocomputing* **2020**, *412*, 320–326. [CrossRef]
28. Zhao, D.; Li, Y.; Li, S.; Cao, Z.; Zhang, C. Distributed Event-Triggered Impulsive Tracking Control for Fractional-Order Multiagent Networks. *IEEE Trans. Syst. Man, Cybern. Syst.* **2022**, *52*, 4544–4556. [CrossRef]
29. Cao, B.; Nie, X. Event-triggered adaptive neural networks control for fractional-order nonstrict-feedback nonlinear systems with unmodeled dynamics and input saturation. *Neural Netw.* **2021**, *142*, 288–302. [CrossRef] [PubMed]

30. Tan, Y.; Xiong, M.; Zhang, B.; Fei, S. Adaptive Event-Triggered Nonfragile State Estimation for Fractional-Order Complex Networked Systems with Cyber Attacks. *IEEE Trans. Syst. Man Cybern. Syst.* **2022**, *52*, 2121–2133. [CrossRef]
31. You, X.; Shi, M.; Guo, B.; Zhu, Y.; Lai, W.; Dian, S.; Liu, K. Event-triggered adaptive fuzzy tracking control for a class of fractional-order uncertain nonlinear systems with external disturbance. *Chaos Solitons Fractals* **2022**, *161*, 112393. [CrossRef]
32. Shahvali, M.; Naghibi-Sistani, M.B.; Askari, J. Dynamic Event-Triggered Control for a Class of Nonlinear Fractional-Order Systems. *IEEE Trans. Circuits Syst. II Express Briefs* **2022**, *69*, 2131–2135. [CrossRef]
33. Yang, W.; Zheng, W.X.; Yu, W. Observer-Based Event-Triggered Adaptive Fuzzy Control for Fractional-Order Time-Varying Delayed MIMO Systems Against Actuator Faults. *IEEE Trans. Fuzzy Syst.* **2022**, *30*, 5445–5459. [CrossRef]
34. Cheng, H.; Huang, X.; Li, Z. Unified neuroadaptive fault-tolerant control of fractional-order systems with or without state constraints. *Neurocomputing* **2023**, *524*, 117–125. [CrossRef]
35. Li, Y.X.; Wei, M.; Tong, S. Event-Triggered Adaptive Neural Control for Fractional-Order Nonlinear Systems Based on Finite-Time Scheme. *IEEE Trans. Cybern.* **2021**, *52*, 9481–9489. [CrossRef]
36. You, X.; Dian, S.; Liu, K.; Guo, B.; Xiang, G.; Zhu, Y. Command Filter-Based Adaptive Fuzzy Finite-Time Tracking Control for Uncertain Fractional-Order Nonlinear Systems. *IEEE Trans. Fuzzy Syst.* **2022**, *31*, 226–240. [CrossRef]
37. Qu, Y.; Ji, Y. Fractional-order finite-time sliding mode control for uncertain teleoperated cyber–physical system with actuator fault. *ISA Trans.* **2024**, *144*, 61–71. [CrossRef] [PubMed]
38. Palanisamy, G.; Kashkynbayev, A.; Rajan, R. Finite-Time Stability of Fractional-Order Discontinuous Nonlinear Systems with State-Dependent Delayed Impulses. *IEEE Trans. Syst. Man, Cybern. Syst.* **2024**, *54*, 1312–1324. [CrossRef]
39. Kavikumar, R.; Kwon, O.M.; Lee, S.H.; Sakthivel, R. Input-output finite-time IT2 fuzzy dynamic sliding mode control for fractional-order nonlinear systems. *Nonlinear Dyn.* **2022**, *108*, 3745–3760. [CrossRef]
40. Xue, G.; Lin, F.; Li, S.; Liu, H. Adaptive fuzzy finite-time backstepping control of fractional-order nonlinear systems with actuator faults via command-filtering and sliding mode technique. *Inf. Sci.* **2022**, *600*, 189–208. [CrossRef]
41. Podlubny, I. *Fractional Differential Equations*; Academic press: Cambridge, MA, USA, 1999; p. 2.
42. Das, S. *Functional Fractional Calculus for System Identification and Controls*; Springer: Berlin/Heidelberg, Germany, 2008.
43. Wang, H.; Chen, B.; Liu, X.; Liu, K.; Lin, C. Robust Adaptive Fuzzy Tracking Control for Pure-Feedback Stochastic Nonlinear Systems with Input Constraints. *IEEE Trans. Cybern.* **2013**, *43*, 2093–2104. [CrossRef]
44. Yu, J.; Shi, P.; Dong, W.; Lin, C. Command Filtering-Based Fuzzy Control for Nonlinear Systems with Saturation Input. *IEEE Trans. Cybern.* **2017**, *47*, 2472–2479. [CrossRef]
45. Beckenbach, E.F.; Bellman, R. *Inequalities*; Cambridge University Press: Cambridge, UK, 1952.
46. Ren, B.; Ge, S.S.; Tee, K.P.; Lee, T.H. Adaptive Neural Control for Output Feedback Nonlinear Systems Using a Barrier Lyapunov Function. *IEEE Trans. Neural Netw.* **2010**, *21*, 1339–1345. [PubMed]
47. Tee, K.P.; Ge, S.S.; Tay, E.H. Barrier Lyapunov Functions for the control of output-constrained nonlinear systems. *Automatica* **2009**, *45*, 918–927. [CrossRef]
48. Wang, L.X. *Adaptive Fuzzy Systems and Control: Design and Stability Analysis*; Prentice-Hall: Englewood Cliffs, NJ, USA, 1994.
49. Duarte-Mermoud, M.A.; Aguila-Camacho, N.; Gallegos, J.A.; Castro-Linares, R. Using general quadratic Lyapunov functions to prove Lyapunov uniform stability for fractional order systems. *Commun. Nonlinear Sci. Numer. Simul.* **2015**, *22*, 650–659. [CrossRef]
50. Aguila Camacho, N.; Duarte Mermoud, M.A.; Gallegos, J.A. Lyapunov functions for fractional order systems. *Commun. Nonlinear Sci. Numer. Simul.* **2014**, *19*, 2951–2957. [CrossRef]
51. Chen, W.; Dai, H.; Song, Y.; Zhang, Z. Convex Lyapunov functions for stability analysis of fractional order systems. *IET Control Theory Appl.* **2017**, *11*, 1070–1074. [CrossRef]
52. Peng, X.; Wu, H.; Cao, J. Global Nonfragile Synchronization in Finite Time for Fractional-Order Discontinuous Neural Networks with Nonlinear Growth Activations. *IEEE Trans. Neural Netw. Learn. Syst.* **2019**, *30*, 2123–2137. [CrossRef]
53. Polycarpou, M.M. Stable adaptive neural control scheme for nonlinear systems. *IEEE Trans. Autom. Control* **1996**, *41*, 447–451. [CrossRef]